Higher Energy Saving with New Heat Integration Arrangement in Heat-Integrated Distillation Column

Toshihiro Wakabayashi
Process Engineering Div., Toyo Engineering Corporation, 2-8-1 Akanehama, Narashino 275-0024, Japan

Shinji Hasebe
Dept. of Chemical Engineering, Kyoto University, Katsura Campus, Nishikyo-ku, Kyoto 615-8510, Japan

DOI 10.1002/aic.14865
Published online May 23, 2015 in Wiley Online Library (wileyonlinelibrary.com)

In conventional heat-integrated distillation columns (HIDiCs), the internal heat exchange is executed between the pressurized rectifying section and the stripping section, which are located at the same elevation. In such a structure, the amount of heat exchanged between two sections depends on the temperature profile of both sections. The resulting enthalpy profile inside the column departs from that in reversible distillation, which is the ideal distillation operation in view of energy conservation. More energy saving may be achieved by providing appropriate arrangement of heat exchanges between sections. The interactive graphical design method to determine the appropriate heat exchange arrangement in a previous paper was developed for a binary system. The design method was extended and applied to a multicomponent system by adopting the idea of a quasi-binary system. Also, a new HIDiC structure that can realize the outcomes of the proposed design method was developed. The economics of the proposed structure was precisely evaluated through a case study of a commercial scale column. It demonstrated that the proposed structure has attractive economics. © 2015 American Institute of Chemical Engineers *AIChE J*, 61: 3479–3488, 2015
Keywords: energy conservation, heat-integrated distillation column, multicomponent, H-xy diagram, graphical design method

Introduction

In view of energy conservation of distillation columns, reversible distillation provides the ultimate figure. The heat-integrated distillation column (HIDiC) attracts considerable attention as its concept is to realize a similar enthalpy profile inside of a column as that in reversible distillation.[1–3] Usually, as a hardware structure, heat exchange between the stripping and rectifying sections at same elevation has been discussed as HIDiC was first proposed by Mah et al.[4] With such pairing of heat exchange, the heat duty at each internal heat exchanger is merely the consequence of the temperature difference of the sections involved in the heat exchange. Accordingly, the heat duty largely depends on the temperature profile of the column, and is fairly different from that of the reversible distillation column.

With respect to the pairing of stages, Gadalla et al.[5] and Olujic et al.[6] reported its effect on energy conservation. However, in those studies, stages were categorized into only a few groups, and the energy conservation was evaluated by changing the combination of heat integration among the groups. Those studies were not based on a theoretical approach and no attempt was made on the cause of the difference in the energy conservation among the combinations. No study was made in terms of the pairing based on stage-wise approach, either. Therefore, there is much room for improvement in the internal heat exchange approach.

Wakabayashi and Hasebe[7] showed that appropriate side heat exchange arrangement gives composition and enthalpy profiles close to the reversible distillation. Here, side heat exchange arrangement is a collective term of (1) composition/stage to add or remove heat, (2) heat duty at each side heat exchanger, and (3) pairing of stages at side heat exchangers. Note that in side heat exchange the condenser and the reboiler are regarded as candidates for heat exchange stages in addition to the internal stages between the rectifying section and the stripping section.

The arrangement of side heat exchangers can be regarded as a combinatorial optimization problem that, Mixed Integer Nonlinear Programming (MINLP) can be used to solve. However, such problem has inherently nonlinear and nonconvex equations which combine continuous variables (such as heat duties of condenser, reboiler and side heat exchangers, compression ratio, etc.) and discrete variables (such as number of theoretical stages, the stages to install the side heat exchanges, those pairing, etc.). Such complexity results in the difficulty of solving the problem and falls in local optima. In fact, most researchers avoid such complex problem by some techniques. Alcantara-Avila et al.[8] linearized the relationship between the effect of side heat exchange duty and the reduction of reboiler duty by introducing a parameter called compensation factor. However, the mutual effect among the plural side heat

Correspondence concerning this article should be addressed to T. Wakabayashi at toshihiro.wakabayashi@toyo-eng.com.

exchanges cannot be formulated exactly. Harwardt and Marquardt[9] and Suphanit[10] limited the pairings of side heat exchange stages to those located at the physically same elevation of the rectifying and the stripping sections. By limiting the pairing, the number of discrete variables can be largely eliminated. However, such limitation reduces the possibility of deriving the best pairing among stages. As described above, MINLP has some limitation in study conditions directly related to the arrangement of side heat exchangers. Another problem in MINLP is its time consuming nature. In industry, the applicability of HIDiC has to be evaluated at conceptual design phase. At such phase, many design parameters, such as number of stages, energy conservation, operating pressure, and so forth have to be studied at the same time. Therefore, MINLP formulation which needs long computational time is not suitable for the study on the screening of the candidates of the arrangement of side heat exchangers.

Accordingly, to study the arrangement of side heat exchangers without any limitation and to study it in limited time such as at conceptual design phase, Wakabayashi and Hasebe[7] proposed a completely new graphical design approach to determine the arrangement of side heat exchangers. The proposed design methodology was limited to a binary system.

In this article, we extended the design methodology developed by the authors for a binary system to a multicomponent system. Moreover, a new HIDiC structure realizing the outcomes of the proposed design methodology was presented. The economics was also evaluated on the newly proposed HIDiC system.

Design Methodology for Binary System

Here, the design methodology developed for the binary system in a previous paper is explained briefly. Then, the way to extend it to a multicomponent system is explained in the next section. The method takes a graphical approach, in which the Ponchon–Savarit *H-xy* diagram is largely modified.

Set the target energy saving by HIDiC to conventional distillation column

The unique feature of the proposed methodology is that the target energy saving with HIDiC to the conventional distillation column is determined in advance, and then the arrangement of side heat exchangers to satisfy it is investigated. When a distillation problem is given, the number of theoretical stages, $N_{\text{T-conv}}$, and the reboiler duty of a conventional distillation column, $Q_{\text{r-conv}}$, are first calculated, taking the fixed and operation costs into account. In referring to $Q_{\text{r-conv}}$ and $N_{\text{T-conv}}$, the reboiler duty, Q_{r}, the compressor power, Ws, and the number of theoretical stages, N_{T}, in HIDiC are decided by design engineers. The operating pressure at the stripping section, P_{S}, in HIDiC is set at this stage. In this research, it is assumed that the heat exchange is not executed at every stage. Thus, the number of heat exchange stages, N_{E}, is also decided.

Provide the ideal side heat exchange arrangement in the stripping section

The ideal relationship between the composition and the enthalpy is that in the reversible distillation. In the reversible distillation condition, the stripping section has an infinite number of stages and the composition change in neighbor stage is infinitesimal. Therefore, the equilibrium line and the operating line are overlapped on *H-xy* diagram and heat is added to each stage to satisfy the enthalpy profile of the reversible distillation. The distillation curve on *H-xy* diagram for such ideal condition is hereafter called the reversible distillation curve, RDC. To draw RDC on an *H-xy* diagram, the equilibrium line of arbitrary composition, for example, $x_{\text{S},j}$, is extended until it comes across $x = x_{\text{B}}$. The enthalpy at $x = x_{\text{B}}$, that is, $h^{\infty}_{\text{S},j}$, on Figure 1, is the enthalpy of bottoms at hypothetical state corresponding to $x_{\text{S},j}$. RDC is the profile of state ($x_{\text{S},j}$, $h^{\infty}_{\text{S},j}$) from bottoms to feed composition.

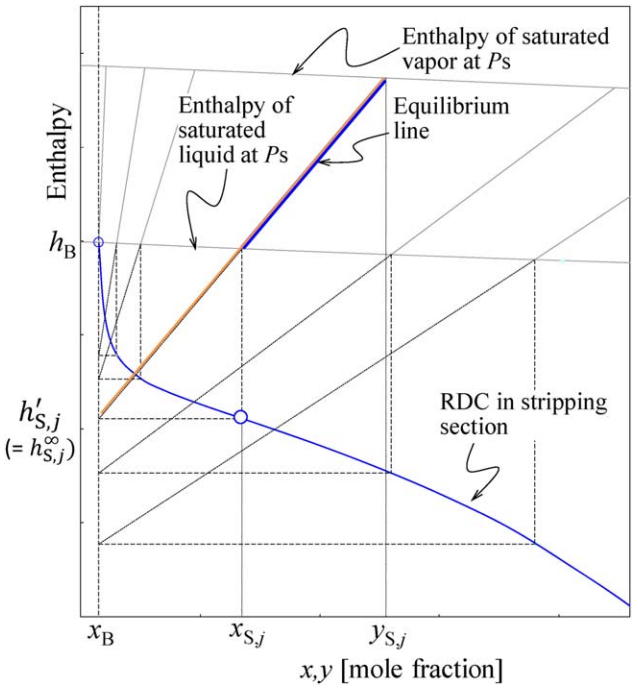

Figure 1. RDC on *H-xy* diagram.

[Color figure can be viewed in the online issue, which is available at wileyonlinelibrary.com.]

Determine the side heat exchange arrangement in the stripping section

The relationship between the liquid composition of the light component and the corresponding hypothetical enthalpy in the actual column is termed the operating locus in the stripping section. First, the ideal operating locus is provided by shifting RDC downward. This curve is the shifted reversible distillation curve, S-RDC (see Figure 2). The distance between RDC and S-RDC is determined so that the number of theoretical stages becomes the prespecified value when the composition change and heat input are given in accordance with that S-RDC. This procedure is accomplished graphically by trial and error manner. Once the location of S-RDC is determined, the operating locus is provided so as to be overlapped with S-RDC. As the limited number of side heat exchangers is given, the operating locus becomes a piecewise flat line. The composition where heat is added and its heat duty, q_k, are adjusted so that the resulting number of stages agrees with the prespecified value. By deciding the operating locus in the stripping section, the heat exchange stages and their compositions and the heat duties for each side heat exchangers are determined.

Provide the ideal side heat exchange arrangement in the rectifying section

Once the operating pressure in the rectifying section, P_{R}, is decided, the equilibrium line and the enthalpy curve of

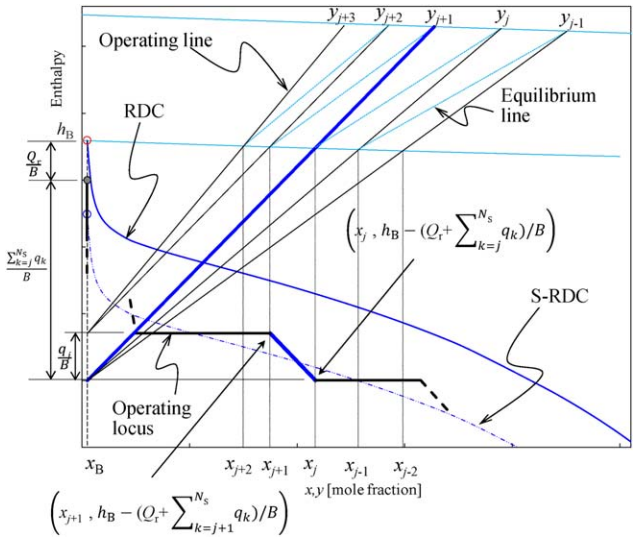

Figure 2. S-RDC and operating locus on *H-xy* diagram.

[Color figure can be viewed in the online issue, which is available at wileyonlinelibrary.com.]

saturated liquid and vapor at P_R can be drawn on the *H-xy* diagram. Then, the RDC in the rectifying section is provided in a similar manner to the stripping section. Thus, in this section, how to decide P_R is explained.

P_R can be calculated using Eq. 1. In Eq. 1, Ws and P_S were already given in a previous step. T_{in} and $\gamma(=c_p/c_v)$, which are the temperature and the ratio of specific heat at compressor inlet, are assumed as those at vapor phase flashed from feed stream under P_S. Accordingly, the undetermined variables in Eq. 1 are P_R and the vapor rate to compressor, V_{in}

$$Ws = \frac{V_{in}}{\eta}\frac{\gamma}{\gamma-1}RT_{in}\left[\left(\frac{P_R}{P_S}\right)^{\gamma-1/\gamma}-1\right] \quad (1)$$

As depicted in Figure 3, V_{in} is the sum of three vapor rates: vapor rate ascending from the top of the stripping section,$V_{S,1}$, the vapor rate flashed from feed stream, F_V, and the vapor rate flashed from liquid descending from the bottom of the rectifying section, $\hat{V}_{R,m}$. $V_{S,1}$ can be calculated from the material and heat balances in the stripping section, and the calculation procedure was explained in the authors' previous work.[7] Once the operating locus has been determined in the stripping section, graphical approach can also be used to decide $V_{S,1}$. F_V can be easily calculated by flash calculation for feed stream under P_S. The remaining term of $\hat{V}_{R,m}$ can be calculated as the result of an iteration process. Here, $\hat{V}_{R,m}$ is once calculated under the assumed P_R, and it is substituted in Eq. 1 to calculate P_R. These steps are repeated until P_R converges.

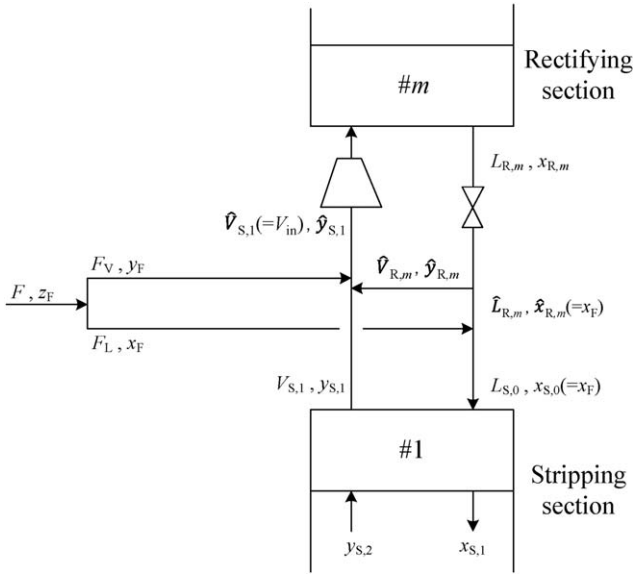

Figure 3. Streams around compressor.

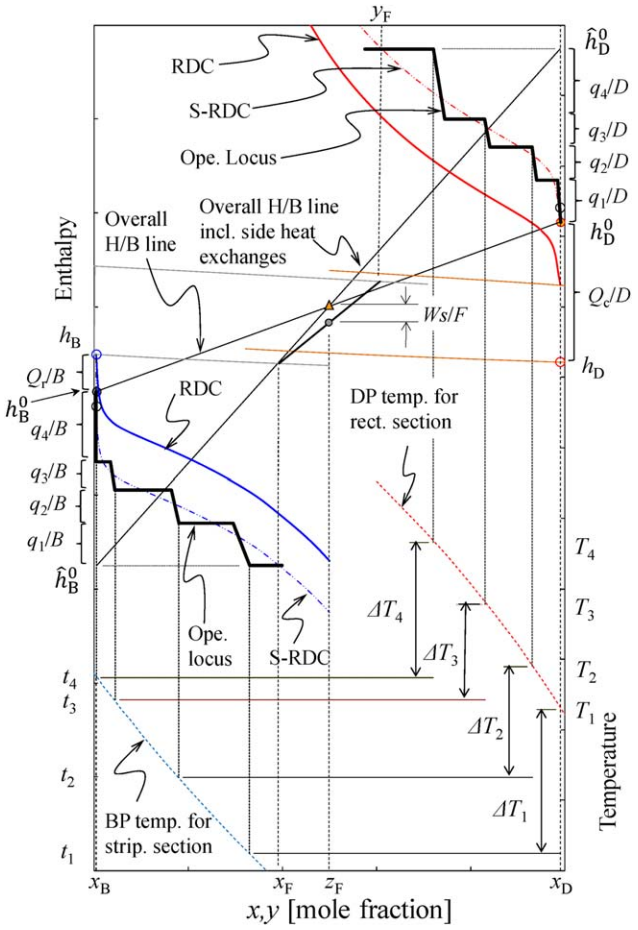

Figure 4. Overview of design methodology on *H-xy* and *T-xy* diagram.

[Color figure can be viewed in the online issue, which is available at wileyonlinelibrary.com.]

Determine the side heat exchange arrangement in the rectifying section

The overall heat balance of HIDiC, including the total heat duties of side heat exchanges, can be shown as a straight line across $(x_B, \hat{h}^0_B)$, $(z_F, h_F + Ws/F)$ and $(x_D, \hat{h}^0_D)$ (See Figure 4). Note that $\hat{h}^0_B$ represents h_B-Q_r/B-$\sum q_k/B$, and $\hat{h}^0_D$ represents $h_D+Q_c/D+\sum q_k/D$. As $\sum q_k$ was already determined through the study in the stripping section, $(x_B, \hat{h}^0_B)$ is known. $(z_F, h_F + Ws/F)$ is also known as Ws is given as a premise. Therefore, $(x_D, \hat{h}^0_D)$ can be uniquely identified. S-RDC in the rectifying section is provided so as to pass through $(y_F, \hat{h}^0_D)$. Thus, the position of S-RDC can be uniquely determined. Besides, each q_k has been already decided in the stripping section. So, the operating locus starting from point (x_D, h^0_D) changes its enthalpy step-wise according to the values of q_k.

Table 1. Process Condition for Case Study

Feed rate	kmol/s	1/18
Feed composition	mol %	
Toluene/Ethylbenzene/ *p*-Xylene/*m*-Xylene/ *o*-Xylene/Cumene/ *n*-propylbenzene/ *m*-Ethyltoluene/ 1,2,4-trimethylbenzene		0.5/10.0/11.0/25.0/ 14.5/1.0/2.2/15.8/20.0
Liquid molar fraction in feed	–	1
Separation specifications		
C9 aromatics in distillate	mol %	0.7
C8 aromatics in bottoms	mol %	1.5
NTS at rect. section and strip. section	–/–	30/25
Pressure drop		
Theoretical stages	kPa/stage	0
Condenser/Reboiler	kPa	0/0
Pressure in strip. section	kPa	101.3

The operating locus should be given so as to overlap with S-RDC. The composition where heat is removed is determined so that the number of theoretical stages meets the prespecified value.

Confirmation of temperature difference of each side heat exchangers

To get the temperature information, the *T-xy* diagram is integrated with the *H-xy* diagram (Figure 4). When the enthalpy curves were provided in a previous step, the temperature has been also available. As the composition where heat is added or removed has been known, the temperature corresponding to that composition can be readily taken from the dew/bubbling point temperature curves.

Heat-transfer area can be calculated by assuming an appropriate heat-transfer coefficient in addition to the temperature difference. If the obtained area is too large to accommodate it in the column diameter, which can be assumed based on the vapor and liquid traffic inside column, the study has to be back to the first step and reset the target energy conservation. If the obtained area is acceptable, the rigorous process simulation is implemented using the outcomes obtained through the graphical method as initial conditions.

Design Methodology for Multicomponent System

The design methodology developed for a binary system is generalized so as to be applied to a multicomponent system. Only the specific points to apply to a multicomponent system are described below.

Calculation of artificial vapor-liquid equilibrium condition and enthalpies

For a binary system, once the liquid concentration of one component is given, the composition and the enthalpy of the vapor at the saturated condition can be identified uniquely. Subsequently, the enthalpy curves at saturated conditions and equilibrium lines can be drawn on an *H-xy* diagram. However, in a multicomponent system the composition and the enthalpy are not determined by the concentration of a single component. When a multicomponent system is discussed, there are several approaches to generate a quasi-binary system and to generate *H-xy* diagram. For the simplicity of explanation, we assume that a multicomponent system consists of components A, B, C, D, and E (in order of bubbling point temperature) and that the key components are C and D.

First, we must decide how the quasi-composition is calculated. In method 1, the liquid fractions of quasi-light key component, x_L, is calculated as total fraction of light nonkey and light key components, that is, $x_L = x_A + x_B + x_C$. In method 2, only the fractions of key components are used to calculate the fractions of quasi-light and quasi-heavy key components, that is, $x_L = x_C/(x_C + x_D)$.[11] The other point is how to define the enthalpy and the vapor-liquid equilibrium (VLE) of the quasi-binary system. In method A, the enthalpy of quasi-light key component is calculated as a weighted average of those of components A, B, and C at the feed condition. The vapor pressure of quasi-light key component is defined as a weighted average of those of components A, B, and C at the feed condition. The vapor pressure of quasi-heavy key component is defined in the same way. Then, the VLE is calculated by Raoult's low. As the weighted average is used, this approach is limited to ideal system. In method B, the properties of only key components are used to calculate the enthalpy and the VLE. In this case, nonideality of the VLE can be embedded in the model. However, this approximation may have large error when the key components do not occupy the majority of the stream. The ratio of light components A, B, and C gradually changes with the stages in the distillation column, and it affects the enthalpy and the VLE. Thus, it is desirable to consider the effect of composition change in the calculation of the enthalpy and the VLE.

By considering this fact, the third method (method C) is proposed in this research. When five components mixture is processed in a continuous distillation column, the liquid compositions on the stages make a trajectory in the four dimensional composition space. As far as the feed composition is the same, the trajectories show similar lines in the four-dimensional space even when the operation condition is changed. Thus, to derive the VLE and the enthalpy of quasi-binary system, a steady-state equilibrium model rigorous simulation that satisfies the product specification is executed for a conventional distillation column with $N_{T\text{-conv}}$ stages under the arbitrary pressure. The obtained liquid and vapor compositions at each stage are divided into two groups using method 1 or method 2.

The proposed procedure was demonstrated through a case study. The process conditions of the case study are given in Table 1, in which the mixture is separated to C8 aromatics (0.7 mol % of C9 aromatics in distillate) and C9 aromatics (1.5 mol % of C8 aromatics in bottoms) under atmospheric pressure, 101.3 kPa. The applicability of two methods, method 1-C and method 2-C, was verified using the case study. The results of two methods to generate the quasi-binary system are shown in Table 2 and Figure 5, in which the data only in the stripping section are shown for clarity. Light key component is *o*-xylene and heavy key component is cumene in this case. These key components occupy only 15.5 mol % in the feed stream, which is quite a small fraction. Bubbling point temperature corresponding to the liquid composition was also provided along with *H-xy* diagram by using right ordinate. As can be seen from Figure 5, the obtained components in the quasi-binary system are considerably different between method 1-C and 2-C. As method 2-C creates quasi-binary system based on only key components, such approach may result in aggressive approximation. This is because the composition change in key component occupying such a small fraction does not always

Table 2. Comparison of Two Methods to Generate Quasi-Binary Component (for Stripping Section Only)

Stage No. in Strip Sect	Temp. (K)	Phase	Enthalpy (kJ/kmol)	Composition in Molar Fraction									Method 1-C		Method 2-C	
				Toluene	Ebz	*p*-Xylene	*m*-Xylene	*o*-Xylene	Cumene	*n*-Propylbz	M3-Ebz	124-Mbz	Light	Heavy	Light	Heavy
S1	420.4	Vapor	67204	0.0034	0.1084	0.1292	0.3018	0.2180	0.0128	0.0176	0.1239	0.0849	0.7609	0.2391	0.9447	0.0553
		Liquid	30632	0.0014	0.0826	0.1041	0.2473	0.2023	0.0145	0.0241	0.1705	0.1532	0.6376	0.3624	0.9329	0.0671
S2	420.7	Vapor	67357	0.0016	0.0980	0.1234	0.2933	0.2376	0.0139	0.0182	0.1275	0.0864	0.7540	0.2460	0.9446	0.0554
		Liquid	30751	0.0007	0.0741	0.0987	0.2386	0.2189	0.0158	0.0247	0.1740	0.1547	0.6309	0.3691	0.9328	0.0672
S3	421.0	Vapor	67513	0.0008	0.0879	0.1171	0.2829	0.2573	0.0154	0.0188	0.1316	0.0882	0.7460	0.2540	0.9436	0.0564
		Liquid	30878	0.0003	0.0660	0.0929	0.2284	0.2352	0.0173	0.0254	0.1783	0.1564	0.6227	0.3773	0.9317	0.0683
S4	421.3	Vapor	67682	0.0004	0.0783	0.1102	0.2708	0.2767	0.0171	0.0197	0.1367	0.0901	0.7364	0.2636	0.9417	0.0583
		Liquid	31021	0.0002	0.0583	0.0867	0.2168	0.2508	0.0191	0.0262	0.1835	0.1584	0.6127	0.3873	0.9293	0.0707
⋮	⋮	⋮	⋮	⋮	⋮	⋮	⋮	⋮	⋮	⋮	⋮	⋮	⋮	⋮	⋮	⋮
S11	425.4	Vapor	69910	1.7E-06	0.0259	0.0534	0.1474	0.3408	0.0424	0.0363	0.2301	0.1237	0.5674	0.4326	0.8894	0.1106
		Liquid	33007	6.1E-07	0.0175	0.0380	0.1067	0.2782	0.0426	0.0436	0.2799	0.1936	0.4403	0.5597	0.8673	0.1327
S12	426.4	Vapor	70467	8.7E-07	0.0207	0.0451	0.1265	0.3281	0.0472	0.0413	0.2572	0.1339	0.5204	0.4796	0.8742	0.1258
		Liquid	33493	3.1E-07	0.0137	0.0314	0.0894	0.2612	0.0463	0.0482	0.3059	0.2039	0.3957	0.6043	0.8494	0.1506
S13	427.5	Vapor	71086	1.2E-06	0.0162	0.0372	0.1061	0.3080	0.0517	0.0468	0.2880	0.1460	0.4674	0.5326	0.8563	0.1437
		Liquid	34021	4.1E-07	0.0104	0.0252	0.0731	0.2387	0.0494	0.0532	0.3342	0.2159	0.3474	0.6526	0.8285	0.1715
S14	428.6	Vapor	71750	1.3E-07	0.0124	0.0299	0.0866	0.2812	0.0554	0.0527	0.3216	0.1602	0.4101	0.5899	0.8355	0.1645
		Liquid	34572	4.6E-08	0.0077	0.0198	0.0581	0.2118	0.0515	0.0583	0.3635	0.2295	0.2974	0.7026	0.8045	0.1955
⋮	⋮	⋮	⋮	⋮	⋮	⋮	⋮	⋮	⋮	⋮	⋮	⋮	⋮	⋮	⋮	⋮
S21	435.4	Vapor	75732	2.1E-10	0.0009	0.0030	0.0097	0.0650	0.0419	0.0751	0.4852	0.3192	0.0786	0.9214	0.6083	0.3917
		Liquid	37462	6.3E-11	0.0005	0.0017	0.0055	0.0416	0.0331	0.0700	0.4672	0.3805	0.0493	0.9507	0.5570	0.4430
S22	436.1	Vapor	76076	4.8E-11	0.0005	0.0020	0.0063	0.0469	0.0359	0.0727	0.4798	0.3558	0.0558	0.9442	0.5664	0.4336
		Liquid	37649	1.4E-11	0.0003	0.0011	0.0036	0.0295	0.0279	0.0665	0.4541	0.4170	0.0345	0.9655	0.5142	0.4858
S23	436.8	Vapor	76383	7.0E-12	0.0003	0.0012	0.0040	0.0327	0.0298	0.0686	0.4643	0.3991	0.0382	0.9618	0.5226	0.4774
		Liquid	37794	2.0E-12	0.0002	0.0007	0.0022	0.0203	0.0228	0.0618	0.4320	0.4600	0.0233	0.9767	0.4704	0.5296
S24	437.5	Vapor	76665	4.4E-14	0.0002	0.0007	0.0024	0.0216	0.0237	0.0630	0.4381	0.4504	0.0249	0.9751	0.4763	0.5237
		Liquid	37903	1.3E-14	0.0001	0.0004	0.0013	0.0132	0.0179	0.0558	0.4006	0.5107	0.0150	0.9850	0.4251	0.5749

Note: Ebz: Ethylbenzene, *n*-Propylbz: *n*-Propylbenzene, M3-Ebz : *m*-Ethyltoluene, 124-MBz : 1,2,4-Trimethylbenzene

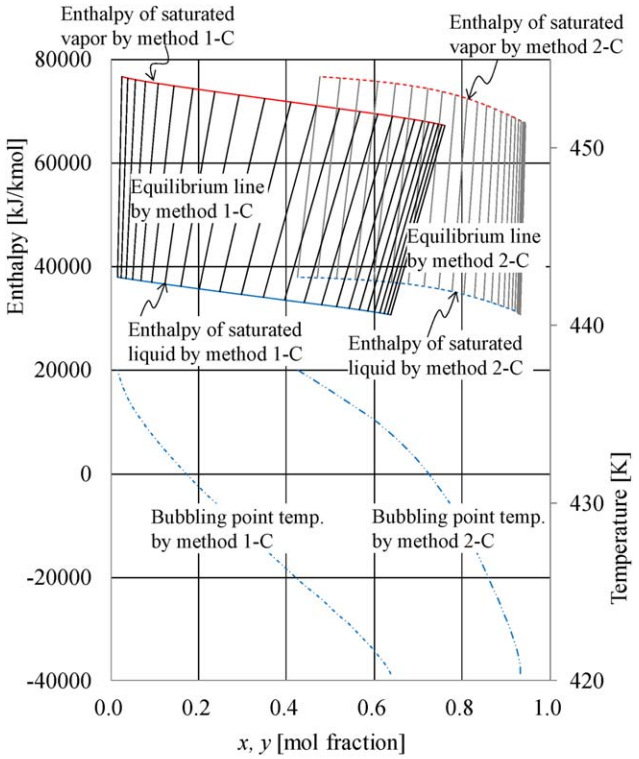

Figure 5. Comparison of two methods to generate the quasi-binary system.

[Color figure can be viewed in the online issue, which is available at wileyonlinelibrary.com.]

represent the majority of component change including nonkey components. In fact, the light key component at stage S1, that is, the stage 1 in the stripping section, in quasi-binary system by method 2-C is 0.9447 and 0.9329 in mole fraction in vapor and liquid phase, respectively. This small difference between vapor and liquid composition results in quite small value of $h^{\infty}_{S,1}$, which is the enthalpy in hypothetical state corresponding to the stage S1 under reversible distillation operation. The enthalpy difference between $h^{\infty}_{S,1}$ and h_B corresponds to the reboiler duty divided by bottoms rate, Q_r/B, at minimum reflux condition. This is well-famous interpretation on H-xy diagram in Ponchon–Savarit diagram. Nevertheless to say, the reboiler duty in actual distillation operation must be larger than that amount. In the case study, (h_B-$h_{S,1}$), that is, Q_r/B in actual operation, is 203,781 kJ/kmol whereas (h_B-$h^{\infty}_{S,1}$) in method 2-C is 1,580,208 kJ/kmol. This is a contradiction on distillation theory as the operating line on Ponshon–Savarit diagram cannot be provided. Conversely, $h^{\infty}_{S,1}$ in method 1-C results in enthalpy difference to h_B of 192,090 kJ/kmol, which does not violate the distillation theory. As illustrated like this, method 2-C cannot create a quasi-binary component appropriately whereas method 1-C can do so. Thus, it can be concluded that method 2-C is inappropriate to represent a quasi-binary system, whereas method 1-C can give appropriate representation for further study. Note that x_B in method 1-C is 0.015, but 0.4251 in method 2-C.

It can also be said that other methods such as methods 1-A, 1-B, 2-A, 2-B do not show better results compared with that of method 1-C. Accordingly, in this research, method 1-C is used to draw the quasi-binary system on an H-xy and T-xy diagram.

Equilibrium conditions, enthalpies of saturated vapor and liquid and bubbling/dew point temperature were obtained at each theoretical stage in a multicomponent system as described above. In the graphical design approach in a multicomponent system, the equilibrium lines to draw operating loci are provided by interpolating the neighbor equilibrium conditions already drawn on the diagram. Operating line can be given just by graphical way. In such manner, RDCs, S-RDCs, and the operating loci can be provided on H-xy diagram. As for the saturated temperature at each stage, it can be read from graph.

When the system contains the intermediate component, that is, the volatility of which is in between two key components, we must decide the treatment of that component. Suppose the case where A and C become key components, and B is the intermediate. In such a case, the following treatment is taken. First, by executing the rigorous process simulation of the conventional column, the flow rate of component B in distillate, D_B, and that in bottoms, B_B, are calculated. Then, for component B the fraction of $D_B/(D_B + B_B)$ is treated as light component and that of $B_B/(D_B + B_B)$ is treated as heavy component. Usually, the concentration of such intermediate component is small. Thus, the simple procedure explained above does not affect the overall quasi-components composition. In case the intermediate component occupies a large fraction, for example, the prefractionator in the distributed sequence, the above procedure is no longer valid, and some limitation exists to apply the proposed method to multicomponent systems.

The procedure to calculate the operating pressure in the rectifying section

Similar to a binary system, the operating pressure in the rectifying section can be assumed. When V_{in} is calculated, P_R has to be determined by iteration procedure using Eq. 1. This is because $\hat{V}_{R,m}$ follows from the flash calculation from P_R to P_S under the assumption of $\hat{y}_{R,m} = y_F$ and $\hat{x}_{R,m} = x_F$. This iteration in a multicomponent can be implemented the same as in a binary system. What is specific in a multicomponent system is that it is difficult to derive $V_{S,1}$ from simple calculation, and it is obtained from the graph where the operating locus in the stripping section is depicted. This is because the VLE of the quasi-binary system is obtained not as a continuous function but as a dataset. In graphical approach, the equilibrium lines and the operating lines can be provided graphically at stage by stage from the bottoms composition, x_B, to the liquid composition of the feed, x_F.

In all other points, the graphical design approach developed for binary systems can be applied to multicomponent systems.

Novel HIDiC Structure to Realize Outcomes of Design Methodology

The side heat exchange arrangement obtained by the design method in the last two sections, which will be clearly demonstrated through a case study in the next section, is quite different from that of the conventional HIDiCs whose structures have basically in parallel set-up between the rectifying section and the stripping section.[2,12] The obtained arrangement has only a limited number of side heat exchangers, and the heat exchange is not executed between the stages at the same elevation. Conversely, with conventional HIDiC structure, the pairing of the stages where side heat exchange is executed cannot be specified but is just a consequence of the parallel set-up of two sections. Also, the discrete allocation of heat duty to side heat exchanges cannot be provided as the heat duty is the

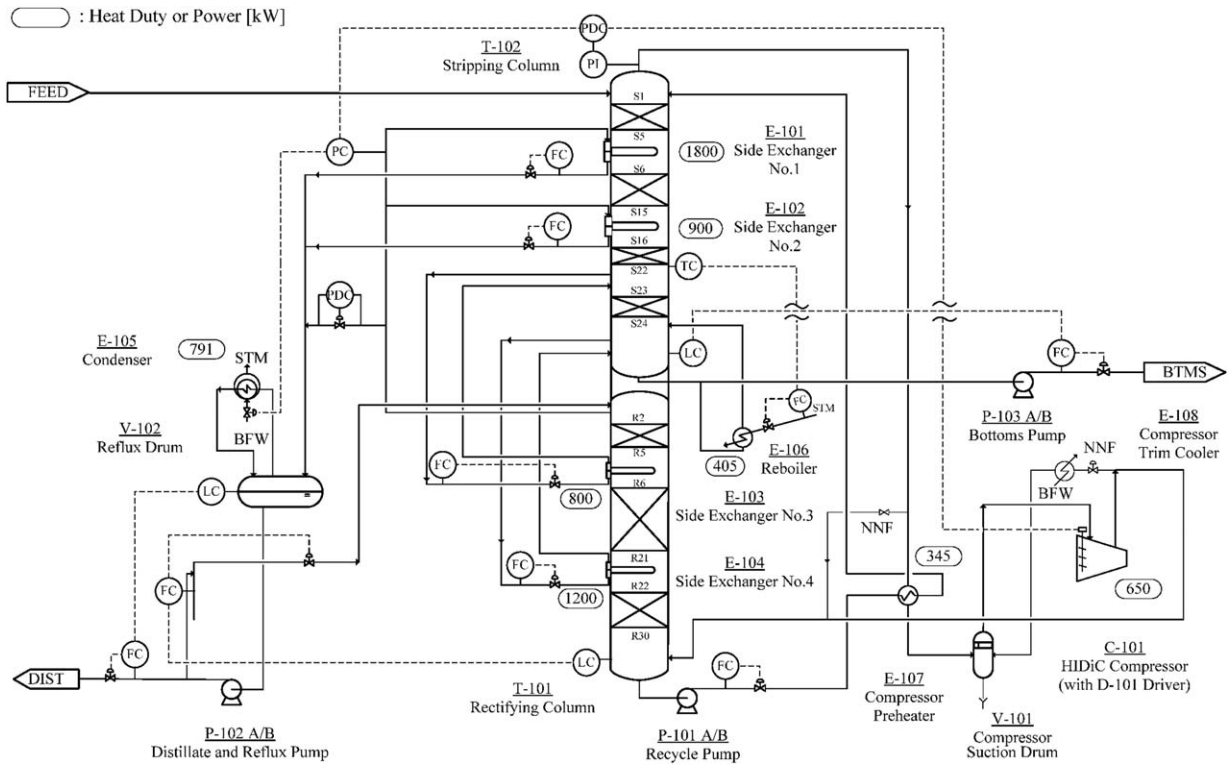

Figure 6. Process flow diagram based on results of case study for new HIDiC structure.

consequence of the temperature difference of the location involved in side heat exchanges and a certain heat-transfer area inherently exist for each side heat exchange. Furthermore, the heat duty cannot be specified with the same reason.

Those characteristics with the proposed method suggest departing from the conventional structure.

To realize the concept, a novel HIDiC structure depicted in Figure 6 was developed (Japan Patent 4803470 and U.S. Patent 8,440,056).[13,14] This new structure consists of well-utilized equipment in industries. For instance, the normal tray/packing is used as column internals, and side heat exchanges are executed by stabbed-in type heat exchangers. What is different from a conventional distillation column is that the low pressure stripping section is elevated above the high pressure rectifying section. With such structure, the following advantages can be realized:

- Side heat exchangers can be installed at the stage/composition where the design method suggests.
- Side heat exchangers can be paired in line with the design results. Such pairing is achievable by installing the stabbed-in type heat exchanger at a decided stage in either the rectifying or the stripping section and by connecting the piping externally from the counter stage to the tube side of the heat exchanger. As the stripping section is located above the rectifying section, the heat exchange can be accomplished by thermosiphon effect or gravity.
- Heat duty of side exchanger can be given in line with the design results. This is because the heat-transfer area of the stabbed-in type heat exchanger can be changed so as to meet the required duty. Thus, the heat duty is not merely dependent on the temperature difference of the paired stages.

Accordingly, the proposed novel structure can have an optimized enthalpy profile inside of the column in maintaining a sufficient temperature difference at side exchanger.

Economics of Proposed HIDiC Structure in Multicomponent System

The economics of the proposed HIDiC was evaluated through a case study (see Table 3). A commercial scale xylene column separates C8 aromatics (0.7 mol % of C9 aromatics in distillate) and C9 aromatics (1.5 mol % of C8 aromatics in bottoms). A conventional distillation column is operated at 106.3 kPa in a reflux drum and at 151.3 kPa at the top of column. The number of theoretical stages, $N_{T\text{-}conv}$, of 55 including reboiler stage and condenser stage, corresponds to 1.15 times larger than the minimum reflux condition in the conventional distillation. The feed stage of 31, counting from the

Table 3. Process Condition for Case Study

Feed rate	kmol/s	1/18
Feed composition	mol %	
Toluene/Ethylbenzene/ *p*-Xylene/*m*-Xylene/ *o*-Xylene/Cumene/ *n*-propylbenzene/ *m*-Ethyltoluene/ 1,2,4-trimethylbenzene		0.5/10.0/11.0/25.0/ 14.5/1.0/2.2/15.8/20.0
Liquid molar fraction in feed	–	1
Separation specifications		
C9 aromatics in distillate	mol %	0.7
C8 aromatics in bottoms	mol %	1.5
NTS at rect. section and strip. section	–/–	30/25
HETP of column packing	m	0.35
Overall heat-transfer coefficient		
Tube bundle in vapor space	kW/(m^{2}K)	0.60
Tube bundle in liquid pool	kW/(m^{2}K)	0.85
Pressure drop		
Theoretical stages	kPa/stage	0.22
Condenser/Reboiler	kPa/kPa	45.0/0.05
Pressure in strip. section	kPa	106.3

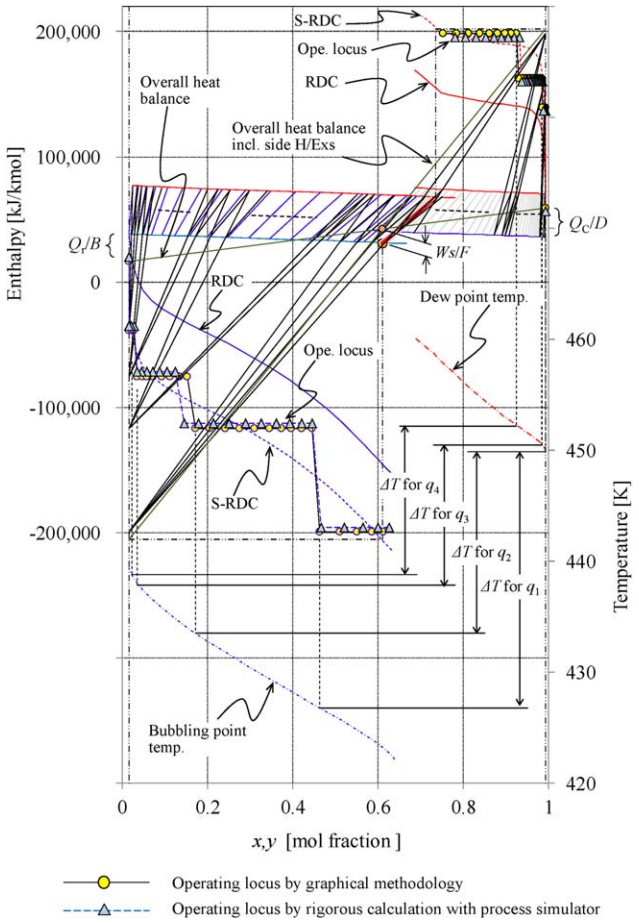

Figure 7. Results of case study on *H-xy* and *T-xy* diagram.

[Color figure can be viewed in the online issue, which is available at wileyonlinelibrary.com.]

condenser stage is optimized in view of energy consumption. Pressure drops in condenser, reboiler, and stages were taken into account in rigorous simulation. Conversely, those were ignored and the operating pressure was set as that at the top of column in the graphical design approach. The reboiler duty of the conventional distillation column, $Q_{\text{r-conv}}$, was 4.78 MW. In the proposed method, the reboiler duty, Q_r, and the target energy saving are decided in advance. In this case study, those were assumed to be 10 and 50% of $Q_{\text{r-conv}}$, respectively. The minimum inlet temperature difference is also an important design variable, and was given as 10 K. The electricity consumed by the compressor is converted into the primary energy with the power generation efficiency of 36.6%. Using this power generation efficiency, the compressor power, *Ws*, of 700 kW subsequently gave the energy conservation of 50.0%. However, with $Q_r = 478$ kW and $Ws = 700$ kW, the lowest temperature difference among side heat exchangers was much larger than 10 K. Thus, further energy saving was considered, that is, *Ws* was reduced to 650 or 600 kW. As the lowest temperature difference among side heat exchangers became smaller than 10 K at *Ws* of 600 kW, *Ws* was decided to be 650 kW. At this condition, the energy conservation of 52.8% was obtained, and this condition was used for further rigorous process simulation step. Here, N_T in HIDiC was set as identical to that in the conventional distillation and N_E was set as four. The operating pressure at the top of the stripping section in HIDiC was set as 106.3 kPa. The steady-state equilibrium model simulator of Pro/II and Soave–Redlich–Kwong equation for properties prediction model was used.

The result of the proposed graphical approach is shown on the *H-xy* and *T-xy* diagram in Figure 7. For operating locus, the result of rigorous calculation is also shown in Figure 7 as triangles. The pairing stages of side heat exchangers and heat duties of each side heat exchanger, q_k, obtained by graphical method were used as initial conditions in rigorous simulation. As can be seen, both results have good agreement especially for the operating loci. The arrangement of side heat exchangers, inlet temperature difference, and heat-transfer area obtained by the design are summarized in Table 4, together with Q_r, *Ws*, and P_R. The obtained Q_r was 405 kW, which is quite similar to the set values. With the given overall heat-transfer coefficient, the heat-transfer area was good enough to be installed in the column diameter based on vapor and liquid traffic inside of the column. The subsequent energy saving was 54.4% for the conventional distillation. The new HIDiC structure to realize the design results was already given in Figure 6.

To evaluate the economics, the total investment cost (TIC) for the new HIDiC system and the conventional distillation system was calculated. With the obtained material/heat balance, the equipment sizes were calculated for both systems. TIC for each system was calculated as per the procedure described by Turton et al.[15] Note that the TIC here corresponds to a grassroots cost in the referenced literature. The parameters to determine the equipment cost are summarized in Table 5 for each piece of equipment in both systems, respectively. As can be seen from Figure 6 and Table 5, equipment such as side heat exchangers, compressor, compressor suction

Table 4. Results of Case Study

Reboiler duty, Q_r					kW	405	(478)
Compressor power, *Ws*					kW	650	(650)
Operating pressure in rectifying section, P_R					kPa	245.4	(249.2)
Side Exchanger Conditions							
	Combination	Duty, q_k (kW)		Inlet Temperature Difference (K)		Heat-Transfer Area, A_k (m^2)	
No. 1	S5-R1	1800	(1800)	23.8	(23.1)	88.9	(91.5)
No. 2	S15-R1	900	(900)	14.4	(16.4)	73.5	(64.6)
No. 3	S22-R6	800	(800)	10.7	(12.7)	115.0	(97.1)
No. 4	S25-R22	1200	(1200)	11.8	(13.4)	156.7	(137.8)

Note: Values in parenthesis are for results in graphical design approach. Heat-transfer area is calculated based on inlet temperature difference but not on log mean temperature difference.

Table 5. Parameters to Determine Equipment Cost

(a) For New HIDiC System

Equipment List

HIDiC having Selective Discrete Side Heat Exchange

Item No.	Service Description	Specifications for Cost Estimation: Parameter	Unit		Material	Remarks
T-101	Rectifying column	Column diameter	mm	2400	KCS	
		Column height	mm	22,920	KCS	
T-102	Stripping column	Column diameter	mm	2400	KCS	
		Column height	mm	23,610	KCS	
T-101P	Packing for T-101	Total bed height	mm	10,150	304 SS	IMTP #15 or equivalent
T-102P	Packing for T-102	Total bed height	mm	8400	304 SS	IMTP #15 or equivalent
C-101	HIDiC compressor	Power	kW	650	CS	Centrifugal
D-101	Compressor driver	Power	kW	650	–	Motor
E-101	Side exchanger No.1	Heat-transfer area	m^2	115	KCS	Stabbed-in
E-102	Side exchanger No.2	Heat-transfer area	m^2	119	KCS	Stabbed-in
E-103	Side exchanger No.3	Heat-transfer area	m^2	177	KCS	Stabbed-in
E-104	Side exchanger No.4	Heat-transfer area	m^2	236	KCS	Stabbed-in
E-105	Condenser	Heat-transfer area	m^2	160	KCS	Fixed type shell and tube type Duty to have 30% of conv. Distillation case for start-up operation
E-106	Reboiler	Heat-transfer area	m^2	160	KCS	Fixed type shell and tube type Duty to have 30% of conv. Distillation case for start-up operation
E-107	Comp'or preheater	Heat-transfer area	m^2	50	KCS	Fixed type shell and tube type
E-108	Comp'or trim cooler	Heat-transfer area	m^2	8	KCS	Fixed type shell and tube type
V-101	Comp'or suction drum	Vessel diameter	mm	2400	KCS	Vertical vessel with demister (304 SS)
		Vessel height	mm	4000	KCS	
V-102	Reflux drum	Vessel diameter	mm	1200	KCS	Horizontal vessel
		Vessel length	mm	3600	KCS	
P-101	Recycle pump	Power	kW	5	CS	Including 1 spare pump
P-102	Dist. and reflux pump	Power	kW	7	CS	Including 1 spare pump
P-103	Bottoms pump	Power	kW	3	CS	Including 1 spare pump

(b) For Conventional Distillation System

Item No.	Service Description	Specifications for Cost Estimation: Parameter	Unit		Material	Remarks
T-201	Column	Column diameter	mm	2300	KCS	
		Column Height	mm	30,000	KCS	
T-201P	Packing for column	Total bed height	mm	18,550	304 SS	IMTP #15 or equivalent
E-201	Condenser	Heat-transfer area	m^2	533	KCS	Fixed type shell and tube type
E-202	Reboiler	Heat-transfer area	m^2	533	KCS	Fixed type shell and tube type
V-201	Reflux drum	Vessel diameter	mm	1300	KCS	
		Vessel height	mm	3900	KCS	
P-201	Dist. and reflux pump	Power	kW	10	CS	Including 1 spare pump
P-202	Bottoms pump	Power	kW	2	CS	Including 1 spare pump

drum, compressor preheater, compressor trim cooler, and recycle pump are additionally required for the new HIDiC system as compared to the conventional distillation system. Conversely, the condenser and reboiler in the new HIDiC system can be smaller than in the conventional distillation system. Note that sizes of these heat exchangers were decided to have 30% of those in the conventional distillation system so as to ease start-up. These values were much larger than the required sizes in a new HIDiC system. In Table 4, the heat-transfer area was calculated using the inlet temperature difference. In cost estimation, the heat-transfer area for each side heat exchanger was calculated on the basis of log mean temperature difference as shown in Table 5. The process scheme for the conventional distillation system was omitted as its scheme is well known.

Under the utility cost of 13 K steam as 30 \$/ton and the electricity as 0.12 \$/kWh, the operating costs (OC) for both systems were calculated as in Table 6. The differences of TIC and OC between the conventional distillation system and the new HIDiC system are expressed by ΔTIC and ΔOC, respectively. From ΔTIC and ΔOC, the payout period was calculated for evaluation. The operating time per year was assumed as 8000 h/year. ΔTIC and ΔOC were 3.46×10^6 \$and 1.30×10^6 \$/year, respectively. Subsequently, ΔTIC/ΔOC was 2.7 years. Such a payout period is well within the criterion in industry of 3 years.

Table 6. OC of New HIDiC and Conventional Distillation

		New HIDiC	Conventional Distillation
Reboiler duty	MW	0.405	4.78
Steam consumption	kg/h	745	8787
Shaft power			
Compressor	kW	650	–
Pumps	kW	15	12
Cost for steam	$\times 10^3$ \$/year	179	2109
Cost for electricity	$\times 10^3$ \$/year	638	12
Total utility cost	$\times 10^3$ \$/year	817	2120

Conclusions

The graphical design methodology which had been proposed in a binary HIDiC system was extended and applied to a multicomponent HIDiC system. In the proposed method, the Ponchon–Savarit *H-xy* diagram was largely modified so that it can be used for heat-integrated systems. To apply it to a multicomponent system, multicomponents were converted into quasi-binary component by classifying the components into two groups. It was confirmed that the side heat exchange arrangement in a multicomponent system could be determined as similar to that in a binary system. In the proposed method, the intermediate process of design can be easily recognized on the graph. Thus, an interactive study on many design parameters can be implemented. This is significantly beneficial to investigating the feasibility of HIDiC in conceptual design phase. Furthermore, a new HIDiC structure was developed, by which the side heat exchange arrangement obtained by the proposed method can be realized. It was demonstrated that the new structure shows attractive economics.

Notation

B = bottoms flow rate, kmol/s
D = distillate flow rate, kmol/s
F = feed flow rate, kmol/s
h = enthalpy per unit molar rate in liquid, kJ/kmol
H = enthalpy per unit molar rate in vapor, kJ/kmol
L = liquid molar flow rate, kmol/s
N_E = number of side exchanges in HIDiC
N_T = number of total theoretical stages including condenser and reboiler
P = pressure, kPa
q = heat duty of side exchanger, kW
Q = heat duty of reboiler or condenser, kW
R = gas constant
t = temperature in stripping section, K
T = temperature in rectifying section, K
V = vapor molar flow rate, kmol/s
Ws = compressor shaft power, kW
x = liquid molar composition of light component
y = vapor molar composition of light component
z = molar composition of light component in mixed phase feed

Subscripts

B = bottoms
C = condenser
D = distillate
F = feed
j = arbitrary stage in stripping section
m = number of theoretical stages in rectifying section
k = serial number of side exchanger
R = rectifying section
r = reboiler
S = stripping section

Literature Cited

1. Nakaiwa M, Huang MK, Endo A, Ohmori T, Akiya T, Takamatsu T. Internally heat-integrated distillation columns: a review. *Chem Eng Res Des*. 2003;81:162–177.
2. Matsuda K, Iwakabe K, Nakaiwa M. Recent advances in internally heat-integrated distillation columns (HIDiC) for sustainable development. *J Chem Eng Jpn*. 2012;45:363–372.
3. Kiss AA, Olujic Z. A review on process intensification in internally heat-integrated distillation columns. *Chem Eng Process*. 2014;86:125–144.
4. Mah RSH, Nicholas JJ, Wodnik RB. Distillation with secondary reflux and vaporization: a comparative evaluation. *AIChE J*. 1977;23:651–658.
5. Gadalla M, Olujic Z, Sun L, de Rijke A, Jansens PJ. Pinch analysis-based approach to conceptual design of internally heat-integrated distillation column. *Chem Eng Res Des*. 2005;83:987–993.
6. Olujic Z, Sun L, Gadalla M, de Rijke A, Jansens PJ. Enhancing thermodynamic efficiency of energy intensive distillation columns via internal heat integration. *Chem Biochem Eng Q*. 2008;22:383–392.
7. Wakabayashi T, Hasebe S. Design of heat integrated distillation column by using H-xy and T-xy diagrams. *Comput Chem Eng*. 2003;56:174–183.
8. Alcantara-Avila JR, Gromez-Castro FI, Segovia-Hernandez JG, Sotowa K, Horikawa T. Optimal design of cryogenic distillation columns with side heat pumps for the propylene/propane separation. *Chem Eng Process*. 2014;82:112–122.
9. Harwardt A, Marquardt W. Heat-integrated distillation columns: vapor recompression or internal heat integration? *AIChE J*. 2012;58:3740–3750.
10. Suphanit B. Optimal heat distribution in the internally heat-integrated distillation column (HIDiC). *Energy*. 2011;36:4171–4181.
11. Hengstebeck RJ. *Distillation Principles and Design Procedures*. Reinhold Publishing Corporation, 1961:107–182.
12. Bruinsma OSL, Krikken T, Cot J, Saric M, Tromp SA, Olujic Z, Standiewicz AI. The structured heat integrated distillation column. *Chem Eng Res Des*. 2012;45:458–470.
13. Nakaiwa M, Wakabayashi T, Tamakoshi A. Jpn Patent 4803470, 2011.
14. Nakaiwa M, Wakabayashi T, Tamakoshi A. U.S. Patent 8,440,056, 2012.
15. Turton R, Bailie RC, Whiting WB, Shaeiwitz JA, Bhattacharyya SD. *Analysis, Synthesis, and Design of Chemical Processes*, 4th ed. New Jersey: Prentice-Hall, 2012.

Manuscript received Dec. 24, 2014, and revision received Apr. 21, 2015.